Inorg. Chem. **2007**, *46*, 839–847

Spectroscopic and Redox Properties of Novel d^6-Complexes Engineered from All *Z*-Ethenylthiophene-bipyridine Ligands

Abdelhalim Belbakra,[†] Sébastien Goeb,[†] Antoinette De Nicola,[†] Raymond Ziessel,*[,†] Cristiana Sabatini,[‡] Andrea Barbieri,[‡] and Francesco Barigelletti*[,‡]

Laboratoire de Chimie Moléculaire, École de Chimie, Polymères, Matériaux (ECPM), Université Louis Pasteur (ULP), 25 rue Becquerel, 67087 Strasbourg Cedex 02, France, and Istituto per la Sintesi Organica e la Fotoreattività, Consiglio Nazionale delle Ricerche (ISOF-CNR), Via P. Gobetti 101, 40129 Bologna, Italy

Received September 25, 2006

A series of quasilinear dinuclear complexes incorporating ruthenium(II)- and osmium(II)-*tris*(2,2′-bipyridine) units has been prepared in which the individual metal-containing moieties are separated by 3,4-dibutyl-2,5-diethenylthiophene spacers and end-capped by 3,4-dibutyl-2-ethenylthiophene subunits; related ruthenium(II) and osmium(II) mononuclear complexes have also been prepared where one bpy unit is likewise end-capped by 3,4-dibutyl-2-ethenylthiophene subunits [bpy = 2,2′-bipyridine]. Overall, mononuclear species, labeled here **Ru** and **Os**, and dinuclear species, **RuRu**, **OsOs**, and **RuOs**, have been prepared and investigated. Their electrochemical behavior has been studied in CH_3CN solvent and reveals ethenylthiophene-centered oxidations (irreversible steps at > +1.37 V vs SCE), metal-centered oxidations (reversible steps at +1.30 V vs SCE for Ru(II/III) and +0.82 V vs SCE for Os(II/III)), and successive reduction steps localized at the substituted bpy subunits. The spectroscopic studies performed for the complexes in CH_3CN solvent provided optical absorption spectra associated with transitions of ligand-centered nature (LC, from the bpy and ethenylthiophene subunits) and metal-to-ligand charge-transfer nature (MLCT), with the former dominating in the visible region (400–600 nm). While the constituent ethenylthiophene-bpy ligands are strong fluorophores (fluorescence efficiency in CH_2Cl_2 solvent, $\phi_{em} = 0.49$ and 0.39, for the monomer and the dimer, respectively), only weak luminescence is observed for each complex in acetonitrile at room temperature. In particular, (i) the complexes **Ru** and **RuRu** do not emit appreciably, and (ii) the complexes **Os**, **OsOs**, and **RuOs** exhibit triplet emission of ^{3}Os → L CT character, with ϕ_{em} in the range from 10^{-3} to 10^{-4}. These features are rationalized on the basis of the role of nonemissive triplet energy levels, ^{3}Th, centered on the ethenylthiophene spacer. These levels appear to lie lower in energy than the ^{3}Ru → L CT triplet levels, and in turn higher in energy than the ^{3}Os → L CT triplet levels, along the sequence ^{3}Ru → L CT > ^{3}Th > ^{3}Os → L CT.

Introduction

Transition metal complexes of ruthenium(II), osmium(II), and rhenium(I), decorated with oligopyridine ligands, have found prominent use in a wide variety of photoactivated molecular systems.[1−9] Most of these materials are luminescent in fluid solution at ambient temperature and have the potential to be used as chemical sensors,[10] electron[8] or photon donors,[11] and light harvesters[12] and to be employed in

* To whom correspondence should be addressed. E-mail: ziessel@chimie.u-strasbg.fr (R.Z.); franz@isof.cnr.it (F.B.).
[†] Université Louis Pasteur.
[‡] Istituto ISOF-CNR.

(1) Juris, A.; Balzani, V.; Barigelletti, F.; Campagna, S.; Belser, P.; von Zelewsky, A. *Coord. Chem. Rev.* **1988**, *84*, 85.
(2) Sauvage, J. P.; Collin, J. P.; Chambron, J. C.; Guillerez, S.; Coudret, C.; Balzani, V.; Barigelletti, F.; Decola, L.; Flamigni, L. *Chem. Rev.* **1994**, *94*, 993−1019.
(3) Harriman, A.; Sauvage, J. P. *Chem. Soc. Rev.* **1996**, *25*, 41.
(4) Harriman, A.; Ziessel, R. *Chem. Commun.* **1996**, 1707−1716.
(5) Ley, K. D.; Whittle, C. E.; Bartberger, M. D.; Schanze, K. S. *J. Am. Chem. Soc.* **1997**, *119*, 3423−3424.
(6) Zhu, S. S.; Kingsborough, R. P.; Swager, T. M. *J. Mater. Chem.* **1999**, *9*, 2123−2131.
(7) Liu, Y.; Li, Y.; Schanze, K. S. *J. Photochem. Photobiol. C: Photochem. Rev.* **2002**, 1−23.
(8) Liu, Y.; De Nicola, A.; Reiff, O.; Ziessel, R.; Schanze, F. S. *J. Phys. Chem. A* **2003**, *107*, 3476−3485.
(9) Chiorboli, C.; Indelli, M. T.; Scandola, F. *Topics Curr. Chem.* **2005**, *257*, 63−102.
(10) Harriman, A.; Hissler, M.; Jost, P.; Wipff, G.; Ziessel, R. *J. Am. Chem. Soc.* **1999**, *121*, 14−27.

10.1021/ic061825y CCC: $37.00 © 2007 American Chemical Society
Published on Web 01/05/2007

electroluminescent devices.[13] In many cases, the photophysical properties of the metal complexes are sensitive to temperature,[14] nuclearity,[15] and nature of the polypyridine ligand.[16] Noteworthy, the attachment of aryl residues[17−20] close to the metal center may provide a means to prolong the triplet lifetime of the complex,[21,22] while the addition of electron-donating or -withdrawing units opens up the possibility of involving the metal complex units in intramolecular electron- and energy-transfer processes.[23−26] Furthermore, the attachment of conjugated substituents to the metal complex introduces the likelihood that ligand-localized excited states will figure in the triplet manifold.[27] Conjugated substituents also favor electron delocalization at the triplet level.[28−30] Thus, several approaches are available for the manipulation of the photophysical properties of these d^6 metal complexes and the assemblies incorporating them.

On the other hand, conjugated materials are prone to playing a significant role in emerging technologies for electronics, optoelectronics, and biotechnology.[31−37] While most applications of conjugated materials that are presently under development are based on organic materials, a number of significant research efforts are focused on the properties of π-conjugated materials that contain transition metals.[7,38−44] Some significant applications that are being considered for metal-containing materials are solid-state electroluminescent devices,[45] organic light-emitting diodes (OLEDs),[46,47−55] laser damage protection,[56,57] and optical signaling.[58]

Oligo- and poly(thiophenes) have been at the forefront of electro- and photoactive conjugated materials research.[59−64] As part of this effort, considerable work has focused on understanding the photophysical properties of thiophene-containing π-conjugated electronic systems.[65−68] Oligo- and

(11) Grosshenny, V.; Harriman, A.; Ziessel, R. *Angew. Chem., Int. Ed. Engl.* **1995**, *34*, 1100−1102.
(12) Kim, C.; Kim, H. *J. Organomet. Chem.* **2003**, *673*, 77−83.
(13) Cunningham, G. B.; Li, Y. T.; Liu, S. X.; Schanze, K. S. *J. Phys. Chem. B* **2003**, *107*, 12569−12572.
(14) Barigelletti, F.; Juris, A.; Balzani, V.; Belser, P.; Von Zelewsky, A. *J. Phys. Chem.* **1986**, *90*, 5190−5193.
(15) Constable, E. C.; Housecroft, C. E.; Schofield, E. R.; Encinas, S.; Armaroli, N.; Barigelletti, F.; Flamigni, L.; Figgemeier, E.; Vos, J. G. *Chem. Commun.* **1999**, 869−870.
(16) Ziessel, R.; Hissler, M.; El-Ghayoury, A.; Harriman, A. *Coord. Chem. Rev.* **1998**, *180*, 1251−1298.
(17) Ford, W. E.; Rodgers, M. A. J. *J. Phys. Chem.* **1991**, *95*, 5827−5831.
(18) Wilson, G. J.; Sasse, W. H. F.; Mau, A. W. H. *Chem. Phys. Lett.* **1996**, *250*, 583−588.
(19) Simon, J. A.; Curry, S. L.; Schmehl, R. H.; Schatz, T. R.; Piotrowiak, P.; Jin, X. Q.; Thummel, R. P. *J. Am. Chem. Soc.* **1997**, *119*, 11012−11022.
(20) Hissler, M.; Harriman, A.; Khatyr, A.; Ziessel, R. *Chem.−Eur. J.* **1999**, *5*, 3366−3381.
(21) Medlycott, E. A.; Hanan, G. S. *Coord. Chem. Rev.* **2006**, *250*, 1763−1782.
(22) McClenaghan, N. D.; Leydet, Y.; Maubert, B.; Indelli, M. T.; Campagna, S. *Coord. Chem. Rev.* **2005**, *249*, 1336−1350.
(23) Del Guerzo, A.; Leroy, S.; Fages, F.; Schmehl, R. H. *Inorg. Chem.* **2002**, *41*, 359−366.
(24) Benniston, A. C.; Harriman, A.; Lawrie, D. J.; Mayeux, A. *Phys. Chem. Chem. Phys.* **2004**, *6*, 51−57.
(25) Baranoff, E.; Collin, J. P.; Flamigni, L.; Sauvage, J. P. *Chem. Soc. Rev.* **2004**, *33*, 147−155.
(26) Kobuke, Y. *Eur. J. Inorg. Chem.* **2006**, 2333−2351.
(27) Walters, K. A.; Premvardhan, L. L.; Liu, Y.; Peteanu, L. A.; Schanze, K. S. *Chem. Phys. Lett.* **2001**, *339*, 255−262.
(28) Benniston, A. C.; Grosshenny, V.; Harriman, A.; Ziessel, R. *Angew. Chem., Int. Ed. Engl.* **1994**, *33*, 1884−1885.
(29) Benniston, A. C.; Goulle, V.; Harriman, A.; Lehn, J. M.; Marczinke, B. *J. Phys. Chem.* **1994**, *98*, 7798−7804.
(30) Grosshenny, V.; Harriman, A.; Romero, F. M.; Ziessel, R. *J. Phys. Chem.* **1996**, *100*, 17472−17484.
(31) Skotheim, T. A., Elsenbaumer, R. L., Reynolds, J. R., Eds. *Handbook of Conducting Polymers*, 2nd ed.; Marcel Dekker: New York, 1998.
(32) McGehee, M. D.; Miller, E. K.; Moses, D.; Heeger, A. J. In *Advances in Synthetic Metals. Twenty Years of Progress in Science and Technology*; Bernier, P., Lefrant, S., Bidan, G., Eds.; Elsevier: Amsterdam, 1999; pp 98−205.
(33) Burroughes, J. H.; Bradley, D. D. C.; Brown, A. R.; Marks, R. N.; Mackay, K.; Friend, R. H.; Burns, P. L.; Holmes, A. B. *Nature* **1990**, *347*, 539−541.
(34) Yu, G.; Gao, J.; Hummelen, J. C.; Wudl, F.; Heeger, A. J. *Science* **1995**, *270*, 1789−1791.
(35) Groenendaal, B. L.; Jonas, F.; Freitag, D.; Pielartzik, H.; Reynolds, J. R. *Adv. Mater.* **2000**, *12*, 481−494.
(36) Chen, L. H.; McBranch, D. W.; Wang, H. L.; Helgeson, R.; Wudl, F.; Whitten, D. G. *Proc. Natl. Acad. Sci. U.S.A.* **1999**, *96*, 12287−12292.
(37) Gaylord, B. S.; Heeger, A. J.; Bazan, G. C. *Proc. Natl. Acad. Sci. U.S.A.* **2002**, *99*, 10954−10957.
(38) Wang, Q.; Yu, L. P. *J. Am. Chem. Soc.* **2000**, *122*, 11806−11811.
(39) Wang, Q.; Wang, L. M.; Yu, L. P. *J. Am. Chem. Soc.* **1998**, *120*, 12860−12868.
(40) Peng, Z. H.; Yu, L. P. *J. Am. Chem. Soc.* **1996**, *118*, 3777−3778.
(41) Ng, P. K.; Gong, X.; Chan, S. H.; Lam, L. S. M.; Chan, W. K. *Chem.−Eur. J.* **2001**, *7*, 4358−4367.
(42) Wilson, J. S.; Dhoot, A. S.; Seeley, A.; Khan, M. S.; Kohler, A.; Friend, R. H. *Nature* **2001**, *413*, 828−831.
(43) Walters, K. A.; Ley, K. D.; Cavalaheiro, C. S. P.; Miller, S. E.; Gosztola, D.; Wasielewski, M. R.; Bussandri, A. P.; van Willigen, H.; Schanze, K. S. *J. Am. Chem. Soc.* **2001**, *123*, 8329−8342.
(44) Walters, K. A.; Dattelbaum, D. M.; Ley, K. D.; Schoonover, J. R.; Meyer, T. J.; Schanze, K. S. *Chem. Commun.* **2001**, 1834−1835.
(45) Slinker, J.; Bernards, D.; Houston, P. L.; Abruna, H. D.; Bernhard, S.; Malliaras, G. G. *Chem. Commun.* **2003**, 2392−2399.
(46) Cyclometalated complexes of Ir(III) have been proven to meet a number of requirements for OLED modeling; however, we give here only a representative list of papers dealing with this family of complexes, see refs 46−53.
(47) Baldo, M. A.; Thompson, M. E.; Forrest, S. R. *Pure Appl. Chem.* **1999**, *71*, 2095−2106.
(48) Baldo, M. A.; O'Brien, D. F.; Thompson, M. E.; Forrest, S. R. *Phys. Rev. B* **1999**, *60*, 14422−14428.
(49) Baldo, M. A.; Lamansky, S.; Burrows, P. E.; Thompson, M. E.; Forrest, S. R. *Appl. Phys. Lett.* **1999**, *75*, 4−6.
(50) Adachi, C.; Baldo, M. A.; Forrest, S. R.; Thompson, M. E. *Appl. Phys. Lett.* **2000**, *77*, 904−906.
(51) Baldo, M. A.; Thompson, M. E.; Forrest, S. R. *Nature* **2000**, *403*, 750−753.
(52) Lamansky, S.; Djurovich, P.; Murphy, D.; Abdel-Razzaq, F.; Lee, H. E.; Adachi, C.; Burrows, P. E.; Forrest, S. R.; Thompson, M. E. *J. Am. Chem. Soc.* **2001**, *123*, 4304−4312.
(53) Lamansky, S.; Djurovich, P.; Murphy, D.; Abdel-Razzaq, F.; Kwong, R.; Tsyba, I.; Bortz, M.; Mui, B.; Bau, R.; Thompson, M. E. *Inorg. Chem.* **2001**, *40*, 1704−1711.
(54) Lamansky, S.; Djurovich, P. I.; Abdel-Razzaq, F.; Garon, S.; Murphy, D. L.; Thompson, M. E. *J. Appl. Phys.* **2002**, *92*, 1570−1575.
(55) Kwong, R. C.; Sibley, S.; Dubovoy, T.; Baldo, M.; Forrest, S. R.; Thompson, M. E. *Chem. Mater.* **1999**, *11*, 3709−3713.
(56) Staromlynska, J.; McKay, T. J.; Bolger, J. A.; Davy, J. R. *J. Opt. Soc. Am. B* **1998**, *15*, 1731−1736.
(57) McKay, T. J.; Staromlynska, J.; Davy, T. R.; Bolger, J. A. *J. Opt. Soc. Am. B* **2001**, *18*, 358−362.
(58) Peng, Z. H.; Gharavi, A. R.; Yu, L. P. *J. Am. Chem. Soc.* **1997**, *119*, 4622−4632.
(59) McCullough, R. D.; Lowe, R. D. *J. Chem. Soc., Chem. Commun.* **1992**, 70−72.
(60) Bäuerle, P.; Fischer, T.; Bidlingmeier, B.; Stabel, A.; Rabe, J. P. *Angew. Chem., Int. Ed. Engl.* **1995**, *34*, 303−307.
(61) Lovinger, A. J.; Rothberg, L. J. *J. Mater. Res.* **1996**, *11*, 1581−1592.
(62) Nishiumi, T.; Higuchi, M.; Yamamoto, K. *Macromolecules* **2003**, *36*, 6325−6332.
(63) Loewe, R. S.; Khersonsky, S. M.; McCullough, R. D. *Adv. Mater.* **1999**, *11*, 250.
(64) Pisignano, D.; Anni, M.; Gigli, G.; Cingolani, R.; Zavelani-Rossi, M.; Lanzani, G.; Barbarella, G.; Favaretto, L. *Appl. Phys. Lett.* **2002**, *81*, 3534−3536.
(65) Kodaira, T.; Watanabe, A.; Ito, O.; Watanabe, M.; Saito, H.; Koishi, M. *J. Phys. Chem.* **1996**, *100*, 15309−15313.

poly(thiophene)s typically feature strong fluorescence from singlet excited states; in addition, direct optical excitation of these systems affords a triplet state in moderate yields.[65−67] In a few cases, phosphorescence has even been observed from polymer samples.[69,70]

Organic π-conjugated electronic systems containing transition metals that interact strongly with the π-electron system are well studied.[5,71−73] For instance, conjugated polymers containing Ru(II) and Os(II) polypyridine complexes interspersed in a poly(3-octylthiophene) backbone, feature energetically low-lying metal-to-ligand charge-transfer (MLCT) excited states, as well as excited states localized on the poly(3-octylthiophene) chain.[74] In this case, photoluminescence and transient absorption studies revealed that for the Ru(II) polymers, the long-lived excited states are primarily of $^3\pi,\pi^*$ character; conversely, for the Os(II) systems, states of MLCT nature are mainly responsible for the photophysics of the materials.

The introduction of vinylene bridges between thiophene moieties improves the electronic properties of the resulting thienylene vinylene polymers[75] and oligomers[76] by decreasing the aromaticity and enhancing planarity.[77] Interestingly, bipyridine units covalently connected to thienylvinylene bridges in Ru(II) complexes and polymers have been proposed as dye sensitizers in solar cells[78] and as chemosensors,[79,80] respectively.

Here, we describe the luminescence properties of a series of elongated arrays end-capped by ethenylthiophene units and containing one and two ruthenium(II)- or osmium(II)-*tris*(2,2′-pyridine) units; ethenylthiophene fragments are also incorporated in the connecting bridge for the dinuclear species (Schemes 1−3). Overall, mononuclear species, **10a** and **10b** (labeled here **Ru** and **Os**, respectively) and dinuclear species, **11a** (**RuRu**), **11b** (**OsOs**), and **12** (**RuOs)** have been prepared and investigated, Chart 1. Prior work[81] has shown that ethynyl bridges facilitate electron exchange between terminal metal complexes, while related research has established that π-conjugated ligands of this general type display interesting electrogenerated luminescence properties.[82−86] In such model systems, it is important to identify the nature of the lowest-energy excited states and to ascertain if individual chromophores operate separately or in a cooperative manner. The results of this study provide insight into how the interplay between ligand-centered (LC) and metal-to-ligand charge-transfer (MLCT) influences the photophysics of the complexes. A short comparison with the behavior of previously reported and closely related ethynyl-containing systems is also provided.[81,87] Hopefully, the information provided by the study of these and similar[81,88,89] systems can prove useful in the design of new metal−organic materials for optoelectronic applications.

Scheme 1[a]

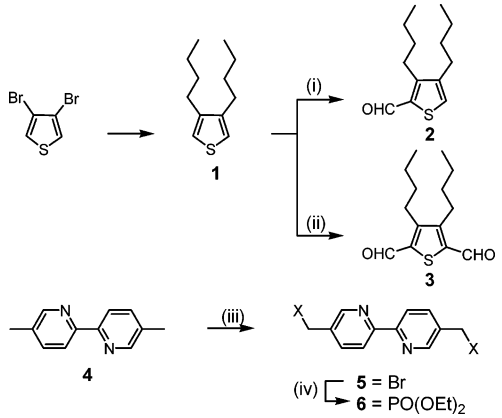

[a] Key: (i) $POCl_3$, anhydrous DMF, anhydrous 1,2-dichloromethane; (ii) TMEDA, ^{n}BuLi, and DMF at −40 °C; (iii) NBS, CCl_4, AIBN, reflux; (iv) neat $PO(OEt)_3$, 125 °C.

Results

Syntheses. The basic strategies employed for synthesizing the target ligands **7** and **9** are based on the Horner−Wadsworth−Emmons ethenylic bond-formation methodology. The synthetic protocol first required the synthesis of the corresponding phosphonate and aldehyde precursors. The preparation of aldehydes **2** and **3** and diphosphonate **6** is depicted in the Scheme 1. The aldehydes were obtained in two steps from commercially available 3,4-dibromothiophene. A Kumada coupling reaction led to the 3,4-dibutylthiophene **1**.[90] The Vilsmeier−Hack formylation[91] of **1** gave mono-

(66) Becker, R. S.; de Melo, J. S.; Macanita, A. L.; Elisei, F. *J. Phys. Chem.* **1996**, *100*, 18683−18695.
(67) de Melo, J. S.; Silva, L. M.; Arnaut, L. G.; Becker, R. S. *J. Chem. Phys.* **1999**, *111*, 5427−5433.
(68) Bennati, M.; Grupp, A.; Mehring, M.; Bauerle, P. *J. Phys. Chem.* **1996**, 100, 2849−2853.
(69) Xu, B.; Holdcroft, S. *Adv. Mater.* **1994**, *6*, 325−327.
(70) Rothe, C.; Hintschich, S.; Monkman, A. P.; Svensson, M.; Anderson, M. R. *J. Chem. Phys.* **2002**, *116*, 10503−10507.
(71) Harriman, A.; Khatyr, A.; Ziessel, R.; Benniston, A. C. *Angew. Chem., Int. Ed.* **2000**, *39*, 4287-+.
(72) Harriman, A.; Mayeux, A.; De Nicola, A.; Ziessel, R. *Phys. Chem. Chem. Phys.* **2002**, *4*, 2229−2235.
(73) Wang, Y. S.; Liu, S. X.; Pinto, M. R.; Dattelbaum, D. M.; Schoonover, J. R.; Schanze, K. S. *J. Phys. Chem. A* **2001**, *105*, 11118−11127.
(74) Walters, K. A.; Trouillet, L.; Guillerez, S.; Schanze, K. S. *Inorg. Chem.* **2000**, *39*, 5496−5509.
(75) Eckhardt, H.; Shacklette, L. W.; Jen, K. Y.; Elsenbaumer, R. L. *J. Chem. Phys.* **1989**, *91*, 1303−1315.
(76) Frere, P.; Raimundo, J. M.; Blanchard, P.; Delaunay, J.; Richomme, P.; Sauvajol, J. L.; Orduna, J.; Garin, J.; Roncali, J. *J. Org. Chem.* **2003**, *68*, 7254−7265.
(77) Wagner, P.; Ballantyne, A. M.; Jolley, K. W.; Officer, D. L. *Tetrahedron* **2006**, *62*, 2190−2199.
(78) Aranyos, V.; Hagfeldt, A.; Grennberg, H.; Figgemeier, E. *Polyhedron* **2004**, *23*, 589−598.
(79) Ding, A. L.; Pei, J.; Yu, W. L.; Lai, Y. H.; Huang, W. *Thin Solid Films* **2002**, *417*, 198−201.
(80) Pei, J.; Ding, A. L.; Yu, W. L.; Lai, Y. H. *Macromol. Rapid Commun.* **2002**, *23*, 21−25.
(81) Goeb, S.; De Nicola, A.; Ziessel, R.; Sabatini, C.; Barbieri, A.; Barigelletti, F. *Inorg. Chem.* **2006**, *45*, 1173−1183.
(82) Noda, T.; Ogawa, H.; Noma, N.; Shirota, Y. *J. Mater. Chem.* **1999**, *9*, 2177−2181.
(83) Mitschke, U.; Bäuerle, P. *J. Mater. Chem.* **2000**, *10*, 1471−1507.
(84) Roncali, J. *Acc. Chem. Res.* **2000**, *33*, 147−156.
(85) Tour, J. M. *Acc. Chem. Res.* **2000**, *33*, 791−804.
(86) Otsubo, T.; Aso, Y.; Takimiya, K. *J. Mater. Chem.* **2002**, *12*, 2565−2575.
(87) Barbieri, A.; Ventura, B.; Flamigni, L.; Barigelletti, F.; Fuhrmann, G.; Bauerle, P.; Goeb, M.; Ziessel, R. *Inorg. Chem.* **2005**, *44*, 8033−8043.
(88) Barbieri, A.; Ventura, B.; Barigelletti, F.; De Nicola, A.; Quesada, M.; Ziessel, R. *Inorg. Chem.* **2004**, *43*, 7359−7368.
(89) Ziessel, R.; Bäuerle, P.; Ammann, M.; Barbieri, A.; Barigelletti, F. *Chem. Commun.* **2005**, 802−804.
(90) Ringenbach, C.; De Nicola, A.; Ziessel, R. *J. Org. Chem.* **2003**, *68*, 4708−4719.

Scheme 2[a]

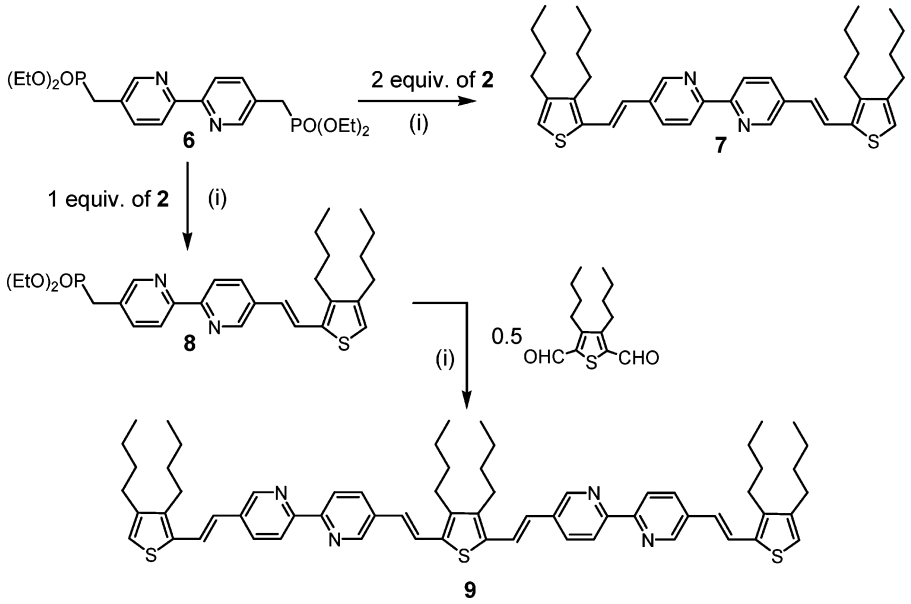

[a] Key: (i) *t*-BuOK, dichloromethane, room temp.

Scheme 3[a]

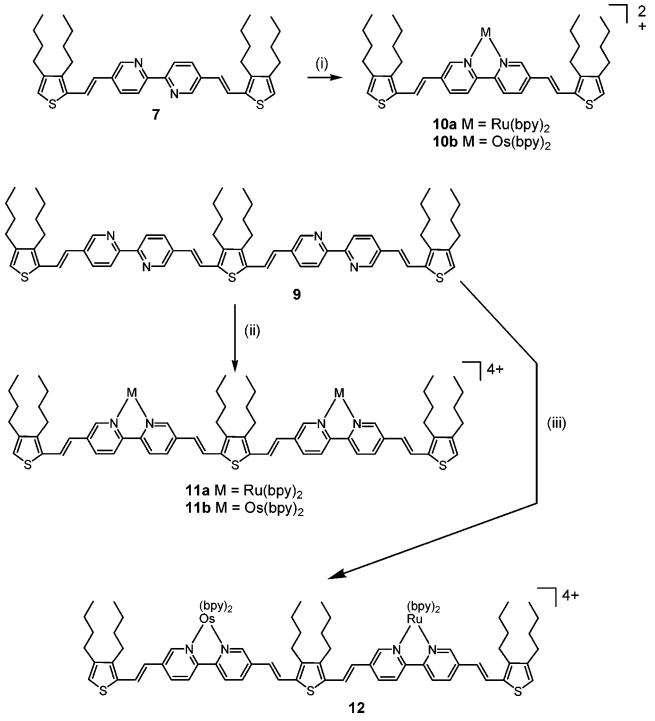

[a] Key: (i) $M(bpy)_2Cl_2$, (1.1 equiv), M = Ru for **10a** and M = Os for **10b**, ethanol, reflux; (ii) $M(bpy)_2Cl_2$ (2.2 equiv), M = Ru for **11a** and M = Os for **11b**, ethanol, reflux; (iii) (a) $[Os(bpy)_2Cl_2]$ (1.0 equiv), ethanol reflux, 48 h, (b) $[Ru(bpy)_2Cl_2]\cdot 2H_2O$ (1.1 equiv), ethanol, reflux, 72 h. In all cases, anion metathesis was insured using KPF_6.

aldehyde **2** in an 84% yield. The dialdehyde **3** was synthesized in a 70% yield by the reaction of **1** with 2.1 equiv of ^{n}BuLi and the subsequent quenching with DMF in the presence of TMEDA.[92] The building block **4**[93] was obtained through self-coupling of 2-bromo-5-picoline catalyzed by Raney Nickel. Bromination of compound **4** with NBS afforded **5**.[94] An Arbuzov reaction on **5** gave the diphosphonate **6**.[58]

Chart 1

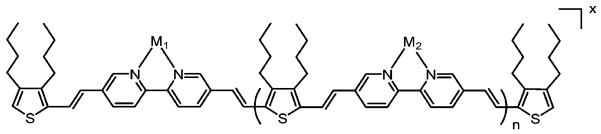

Compounds	n	M_1	M_2	x
7 (monomer)	0	-	-	0
10a (**Ru**)	0	$Ru(bpy)_2$	-	+2
10b (**Os**)	0	$Os(bpy)_2$	-	+2
9 (dimer)	1	-	-	0
11a (**RuRu**)	1	$Ru(bpy)_2$	$Ru(bpy)_2$	+4
11b (**OsOs**)	1	$Os(bpy)_2$	$Os(bpy)_2$	+4
12 (**RuOs**)	1	$Ru(bpy)_2$	$Os(bpy)_2$	+4

Scheme 2 illustrates the synthetic sequences for the synthesis of the final ligands **7** and **9**. Ligand **7** and compound **8,** the key precursor of **9**, were prepared in 96 and 49% yields, respectively, with the same protocol used for aldehyde **2** and the bipyridine diphosphonate **6** in THF by slow addition of *t*-BuOK as base. The formation of the monophosphonate **8** required 1 equiv of **2** and *t*-BuOK, whereas the preparation of **9** required 2 equiv of base and 2 equiv of aldehyde. Like typical Wittig-type reactions, **8** was obtained as a mixture of *E*- and *Z*-vinylene isomers. Only one diastereoisomer, ZZ, was isolated for ligand **7**. The condensation between dialdehyde **3** and **8** under the same conditions gave the ligand **9**. Again, only the all-Z diastereoisomer **9** was obtained with an 84% yield. The stereochem-

(91) Elandaloussi, E. H.; Frere, P.; Richomme, P.; Orduna, J.; Garin, J.; Roncali, J. *J. Am. Chem. Soc.* **1997**, *119*, 10774−10784.
(92) Feringa, B. L.; Hulst, R.; Rikers, R.; Brandsma, L. *Synthesis* **1988**, 316−318.
(93) Sasse, W. H. F. *J. Chem. Soc.* **1959**, 3046.
(94) Ebmeyer, F.; Vogtle, F. *Chem. Ber.* **1989**, *122*, 1725−1727.

Table 1. Electrochemical Data for the Monomer, Dimer, Ruthenium, Osmium, and Appropriate Reference Complexes[a]

	$E^{0,}$ (ox, soln) (V), ΔE (mV)	$E^{0,}$ (red, soln) (V), ΔE (mV)
7 (monomer)	+1.42 (irrev), +1.16 (irrev)	−1.81 (irrev)
10a (Ru)	+1.48 (irrev), +1.30 (60)	−1.03 (70), −1.39 (60), −1.62 (70)
10b (Os)	+1.49 (irrev), +0.82 (70)	−1.11 (70), −1.41 (70), −1.68 (70)
9 (dimer)	+1.39 (irrev), +1.12 (irrev)	−1.63 (90)
11a (RuRu)	+1.38 (irrev), +1.30 (70)	−1.04 (60), −1.48 (60), −1.70 (70)
11b (OsOs)	+1.38 (irrev), +0.83 (70)	−1.05 (60), −1.35 (80), −1.74 (70)
12 (RuOs)	+1.37 (irrev), +0.82 (80)	−1.04 (60), −1.45 (50), −1.71 (irrev)*
$[Ru(bpy)_3]^{2+}$	+1.27 (60)	−1.35 (60), −1.54 (70), −1.79 (70)
$[Os(bpy)_3]^{2+}$	+0.83 (60)	−1.25 (60), −1.44 (70), −1.73 (70)

[a] Potentials determined by cyclic voltammetry in deoxygenated CH_3CN solution, containing 0.1 M $TBAPF_6$, at a solute concentration of ~1 mM and at 20 °C. Potentials were standardized vs ferrocene (Fc) as internal reference and converted to the SCE scale assuming that $E_{1/2}(Fc/Fc^+) = +0.38$ V ($\Delta E_p = 60$ mV) vs SCE. The error in half-wave potentials is ±15 mV. For irreversible processes, the peak potentials (E_{ap} or E_{cp}) are quoted (marked with asterisk). The irreversibility is likely the result of severe adsorption of the complex on the electrolyte surface. All reversible redox steps result from one-electron processes for the mononuclear complexes and two-electron processes for the dinuclear complexes, unless otherwise specified.

istry of the two ligands is likely explained by the photoisomerization Z/E of the double bounds. As the conjugation increases with the size of the ligands, the absorption spectra show the expected red shift assigned to a low-lying π,π^* absorption.[95] We assumed that this weakly energetic transition might facilitate the isomerization of the E alkene to the thermodynamically more stable Z isomer.

The Ru and Os complexes (Scheme 3) were prepared with the procedure that we used previously for the synthesis of d^6 transition metal bipyridine complexes.[81,88] Complexes **10** and **11** were obtained by reaction between ligands **7** or **9** and *cis*-Cl-$[Ru(bipy)_2Cl_2]\cdot 2H_2O$[96] or *cis*-Cl-$[Os(bipy)_2Cl_2]$[97] in ethanol at 90 °C. For the ditopic ligand, unavoidable mixtures of mono- and binuclear complexes could be separated by chromatography on alumina. In all the cases, the complexation with Ru gave better results than with Os. So the preparation of the heteronuclear complex **12** was carried from the mononuclear Os complex of ligand **9** with 69%.

Electrochemistry. The electrochemical properties of the complexes were characterized by cyclic voltammetry in CH_3CN solution. Table 1 lists the potentials (relative to the SCE reference electrode) for the waves that were observed in the +1.6 to −2.0 V window. First, the two free ligands, **7** (monomer) and **9** (dimer), Chart 1, are redox active exhibiting ethenylthiophene-based oxidation at 1.42 and 1.39 V, respectively (irreversible for both of them),[98] and bipyridine reduction (irreversible for **7**, reversible for **9**) at very cathodic potentials, −1.81 and −1.63 V, respectively.[81] Notice that in the monomer **7**, the thiophene units are oxidized at different potentials (1.42 and 1.16 V, separation 260 mV), and for the dimer **9**, the separation of the two potentials at 1.39 and 1.12 V is 270 mV. The reduction is facilitated for the dimer versus the monomer, likely because of a better stabilization of the emergent radical anion for the former case.

The monomeric Ru complex **10a** (**Ru**), Chart 1, exhibits a Ru(II/III) oxidation at +1.30 V, and the monomeric Os complex **10b** (**Os**) has an Os(II/III) oxidation at +0.82 V. In both complexes, a further irreversible oxidation is found at higher potentials (1.48 and 1.49 V, respectively), but it is close to the ethenylthiophene-based oxidation observed for the free ligand **7** (1.42 V), which suggests the same assignment. For the reduction steps for **Ru** and **Os**, in line with previous observations on related compounds,[81] the successive reversible reductions are bipyridine-based with the first step likely located on the substituted bipyridine.

Regarding **11a** (**RuRu)** and **11b** (**OsOs)**, Chart 1, single Ru(II/III) and Os(II/III) waves are found at 1.30 and 0.83 V, respectively, the same potentials observed for the mononuclear complexes, **Ru** and **Os**. The observation of a single metal-centered wave supports the notion that the metal centers of the dinuclear species are not interacting significantly (within a 20 mV range, the typical uncertainty for electrochemical measurements). The same line of reasoning holds for the thiophene-based oxidation steps, occurring at 1.38 V (irreversible) in both **RuRu** and **OsOs** cases.

In the absence of a large interaction between metal centers, the heterodinuclear complex **12** (**RuOs)**, Chart 1, is expected to exhibit two oxidation waves because of the different metal centers. Actually, for this complex, two waves are registered, at 1.37 (irreversible) and 0.82 V. The latter corresponds well to the metal-centered potential observed for the monomeric **Os** and dimeric **OsOs** complexes and also for $[Os(bpy)_3]^{2+}$ (Table 1). For **RuOs**, the (irreversible) wave at 1.37 V is probably an envelop of metal (ruthenium)-centered and thiophene-centered processes, as suggested by comparison with potentials listed in Table 1: 1.27 V for the $[Ru(bpy)_3]^{2+}$ reference complex, 1.30 for both **Ru** and **RuRu**, and (irreversible) potentials larger than 1.37 V in these species, attributed to ethenylthiophene-centered steps (see above).

For all dinuclear species examined, the successive reversible reductions found are bipyridine-based, with the first step likely localized on the substituted bipyridine units, as already discussed for the mononuclear cases, in line with previous results.[81]

Absorption and Luminescence Properties. The absorption and luminescence spectra of the ligands **7** and **9** and of their complexes are displayed in Figures 1 and 2, respectively, and the corresponding data are collected in Table 2. The absorption spectra of **7** and **9** are in agreement with those of previously investigated ligands containing bpy and

(95) Snyder, J. J.; Tise, F. P.; Davis, R. D.; Kropp, P. J. *J. Org. Chem.* **1981**, *46*, 3609−3611.
(96) Sullivan, B. P.; Salmon, D. J.; Meyer, T. J. *Inorg. Chem.* **1978**, *17*, 3334−3341.
(97) Kober, E. M.; Caspar, J. V.; Sullivan, B. P.; Meyer, T. J. *Inorg. Chem.* **1988**, *27*, 4587−4598.

(98) This result is in contrast with the absence of redox activity when the double bonds are replaced by triple bonds, see refs 81 and 88.

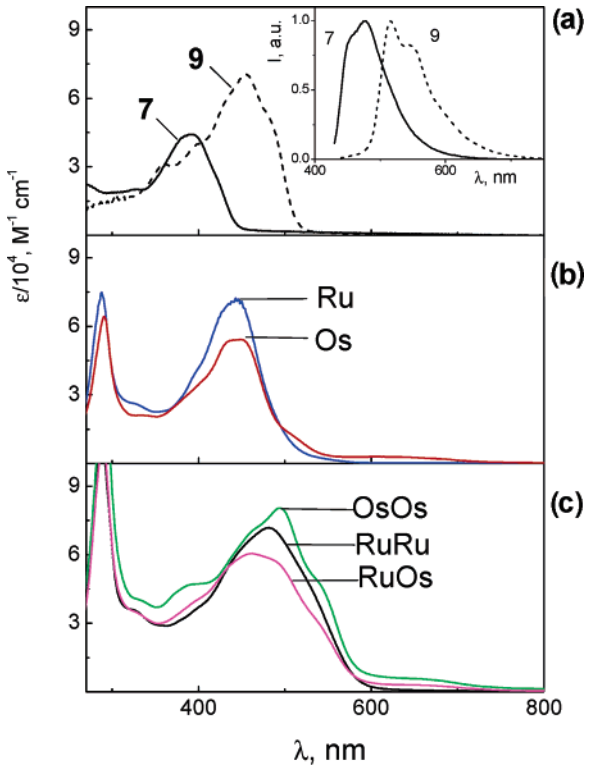

Figure 1. Ground state absorption spectra for ligands **7** and **9** (a; the inset shows room temp luminescence spectra, λ_{exc} = 400 nm), complexes **Ru** and **Os** (b), and complexes **RuRu**, **OsOs,** and **RuOs** (c). The solvents were CH_2Cl_2 for the ligands and CH_3CN for the complexes.

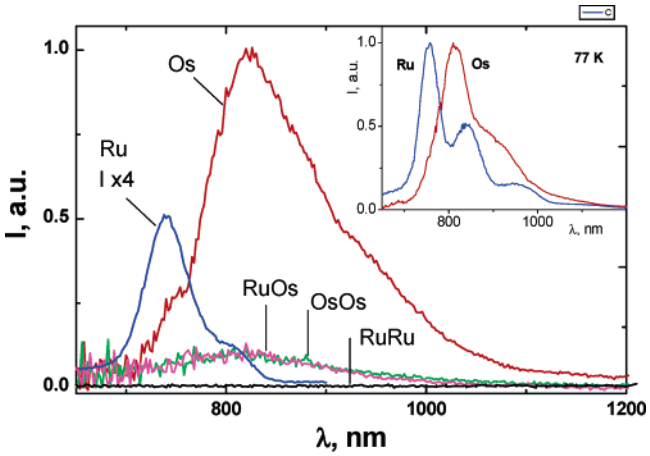

Figure 2. Room-temperature luminescence spectra of isoabsorbing samples of the indicated complexes, λ_{exc} = 450 nm, solvent CH_3CN. The inset shows normalized spectra obtained at 77 K.

thiophene units separated by ethene bridges.[99] The larger size of **9** with respect to **7** is expected to result in a more extended conjugation. Actually, the lowest-energy band peaks at 398 (ϵ = 47 000 M^{-1} cm^{-1}) and 454 nm (ϵ = 70 600 M^{-1} cm^{-1}) for **7** and **9**, respectively, and is likely to include both $^1\pi\pi^*$ transitions at the ethenylthiophene backbone and ^{1}CT transitions involving the alkyl-thiophene groups as donors and the ethenyl-bipyridine residues as acceptors.[99] Conversely, the typical bpy-localized $^1\pi\pi^*$-transition bands, appearing in the range of 280−290 nm, are weak in both **7** and **9** (ϵ < 20 000 M^{-1} cm^{-1}, see Figure 1 panel a), and strong (ϵ in the range of 10^5 M^{-1} cm^{-1}, see Figure 1 panels b and c) in the complexes (see Table 2). Of course, this is the result of the larger number of unsubstituted bpy units in the complexes.

Table 2. Absorption and Luminescence Properties of the Ligand and Complexes[a]

	absorption	emission			
	λ_{max} (nm), ϵ_{max} (M^{-1} cm^{-1})	λ_{em} (nm)	ϕ_{em}	τ (ns)[b]	k_r[c]
7 (monomer)	398 (47 000)	478	0.49	0.90	5.4×10^8
10a (Ru)	288 (74 800), 444 (71 000)	742	1.2×10^{-4}	145	8.3×10^2
10b (Os)	290 (64 300), 444 (54 200), 645 (2600)	822	2.5×10^{-3}	21	1.2×10^5
9 (dimer)	454 (70 600)	516	0.39	1.2	3.3×10^8
11a (RuRu)	290 (108 000), 482 (71 800)	*d*	*d*	*d*	
11b (OsOs)	290 (134 000), 494 (80 500), 645 (5800)	822	3.4×10^{-4}	22.3	1.5×10^4
12 (RuOs)	290 (107 500), 460 (60 500), 645 (3000)	822	3.9×10^{-4}	27.3	1.5×10^4
$[Ru(bpy)_3]^{2+}$*e*	288 (76 600), 452 (14 600)	615	1.5×10^{-2}	170	8.8×10^4
$[Os(bpy)_3]^{2+}$*f*	290 (78 000), 478 (11 100), 579 (3300)	743	3.2×10^{-3}	49	6.5×10^4

[a] Room temperature, air-equilibrated solvents: CH_2Cl_2 for ligands and CH_3CN for complexes. For the ligands, λ_{exc} = 400 nm for the luminescence spectra and 373 nm for the lifetimes; for the complexes, λ_{exc} = 450 and 407 nm, respectively. [b] Values obtained by monitoring the luminescence peak; single-exponential decays were observed in all cases. [c] $k_r = \phi/\tau$. [d] Too weak to be detected. [e] From refs 1 and 100. [f] From refs 102 and 101.

In Figure 1, the absorption profiles of ligands **7** and **9** are compared with those of the derived mononuclear species, **Ru** and **Os**, and the binuclear species **RuRu**, **OsOs**, and **RuOs**. For **Ru** and **Os**, the intensity of bpy-centered $^1\pi\pi^*$ transitions in the 280−290 nm region is comparable to that exhibited by the reference species $[Ru(bpy)_3]^{2+}$ and $[Os(bpy)_3]^{2+}$ in the same region (Table 2), and it increases for the binuclear species examined, as expected because of the increased number of bpy units. For **Ru** and **Os**, the lowest-energy absorption peak is red shifted and more intense (444 nm, with ϵ = 70 100 and 54 200 M^{-1} cm^{-1}, respectively) with respect to ligand **7** (398 nm, ϵ = 47 000 M^{-1} cm^{-1}). For **Ru** and **Os**, these absorption features are attributable to a mixing of the ^{1}MLCT transitions (typically, with ϵ in the range of 10 000−20 000 M^{-1} cm^{-1}, [1,100−102]and more intense ethenylthiophene-centered transitions (likely a combination of $^1\pi\pi^*$ and intraligand ^{1}CT transitions).[81,99] For **Os**, an additional absorption tail extending to 700 nm and more (peaking at 645 nm, ϵ = 2600 M^{-1} cm^{-1}) is also registered, resulting from the (formally forbidden) ^{3}MLCT absorption transitions.[102]

(99) Goeb, S.; De Nicola, A.; Ziessel, R. *J. Org. Chem.* **2005**, *70*, 1518−1529.
(100) Balzani, V.; Bardwell, D. A.; Barigelletti, F.; Cleary, F. L.; Guardigli, M.; Jeffery, J. C.; Sovrani, T.; Ward, M. D. *J. Chem. Soc., Dalton Trans.* **1995**, 3601−3608.
(101) De Cola, L.; Balzani, V.; Barigelletti, F.; Flamigni, L.; Belser, P.; Von Zelewsky, A.; Frank, M.; Vögtle, F. *Inorg. Chem.* **1993**, *32*, 5228−5238.
(102) Kober, E. M.; Caspar, J. V.; Lumpkin, R. S.; Meyer, T. J. *J. Phys. Chem.* **1986**, *90*, 3722−3734.

The absorption spectra for the homometallic binuclear species, **RuRu** and **OsOs**, and the heterometallic species, **RuOs**, Figure 1 panel c, feature intense bands resulting from both (i) transitions centered at the bpy units (around 288−290 nm, with ϵ in the range of 10^5 M^{-1} cm^{-1}) and (ii) overlapping transitions in the 460−494 nm region with $\epsilon \approx$ 60 500−80 500 M^{-1} cm^{-1}. For the mononuclear cases **Ru** and **Os**, despite the higher nuclearity for the binuclear complexes, a comparison of the absorption properties with those for the reference complexes $[Ru(bpy)_3]^{2+}$ and $[Os(bpy)_3]^{2+}$ (Table 2) and for ligand **9** (Figure 1) suggests that for **RuRu, OsOs**, and **RuOs**, the intense band in the region of 460−494 nm is largely centered on the ethenylthiophene fragments.

For the Os-containing binuclear complexes **OsOs** and **RuOs**, an absorption tail of ^{3}MLCT nature extending to 700 nm is also present (ϵ = 5800 and 3000 M^{-1} cm^{-1}, respectively), in agreement with that observed for the mononuclear complex **Os** (see Figure 1 and Table 2).

Luminescence results are gathered in Table 2. Room-temperature luminescence spectra for ligands **7** and **9** are shown in the inset of Figure 1, panel a; room-temperature luminescence spectra for the mononuclear and binuclear complexes are displayed in Figure 2 with the inset showing selected 77 K cases: excitation was performed at 400 or 450 nm (for the ligands and complexes, respectively). The ligands exhibit room-temperature luminescence features (for **7**, λ_{em} = 478 nm, ϕ_{em} =0.49, and τ = 0.9 ns; for **9**, λ_{em} = 516 nm, ϕ_{em} =0.39, and τ = 1.2 ns, in CH_2Cl_2 solvent) that are typical for the fluorescence of thiophene-based oligomers.[66,70,74,81,103,104] As noted above in the discussion of the absorption properties for **7** and **9**, the extended conjugation for the latter results in a red shift for the emission.

For all of the complexes investigated, the intense oligothiophene-based fluorescence exhibited by ligands **7** and **9** disappears and is replaced by a much weaker luminescence, Table 2. In the following, we discuss the luminescence features of the complexes starting with the mononuclear complexes **Ru** and **Os** as compared with the reference complexes $[Ru(bpy)_3]^{2+}$ and $[Os(bpy)_3]^{2+}$.

A first observation is that the luminescence intensities of **Os** and $[Os(bpy)_3]^{2+}$ are comparable, $\phi = 2.5 \times 10^{-3}$ and 3.2×10^{-3}, [101,102] respectively (air-equilibrated CH_3CN solvent). For $[Os(bpy)_3]^{2+}$, light absorption (at 450 nm) leads to a population of ^{1}MLCT levels, and the emission is always from the lowest-lying ^{3}Os → L CT level (λ_{em} = 743 nm, Table 2), because of a very efficient intersystem crossing step ($\phi_{ISC} \approx 1$, an effect of the high spin−orbit coupling constant of the heavy Os center, ζ_{Os} = 3381 cm^{-1}).[105] For **Os**, the use of light at 450 nm is expected to predominantly populate ethenylthiophene-centered excited levels, see discussion above of the absorption features. However, both the luminescence quantum yield and lifetime are similar to those of $[Os(bpy)_3]^{2+}$, which suggests an ^{3}Os → L CT emitting level for **Os**. Of course, the emission peak is lower in energy for **Os** than for $[Os(bpy)_3]^{2+}$ (λ_{em} = 822 and 743 nm, respectively, Table 2), as expected because of the larger conjugation of the ethenylthiophene-bipyridine ligand with respect to bpy.

In contrast, some emission features of **Ru** are quite different from those of $[Ru(bpy)_3]^{2+}$, Table 2; in particular, the luminescence quantum yield is 2 orders of magnitude lower, $\phi_{em} = 1.2 \times 10^{-4}$ vs 1.5×10^{-2}. This can likely be explained by consideration of the role of the ethenylthiophene-centered singlet and triplet levels, ^{1}Th and ^{3}Th, as discussed below.

From the emission maxima listed in Table 2, the ^{1}Th levels for **7** and **9** are determined to lie at 2.6 and 2.4 eV, respectively. The ^{3}Th levels are not luminescent,[65−68] and a direct assessment of their energy level is not easily accomplished. Estimates place their energy at about 0.5−0.7 eV below the corresponding singlet levels, ^{1}Th;[74] accordingly, the ^{3}Th level for **7** and **9** could lie at ∼2 and 1.8 eV, respectively. In conclusion, for **Ru**, it seems that a triplet level of ligand-centered nature (^{3}Th, not emissive) is isoenergetic or even lower in energy than the ^{3}(Ru → L CT) level. Interconversion processes involving the metal- and ligand-centered levels[89] are therefore likely to explain the much-reduced ^{3}MLCT luminescence intensity of **Ru** with respect to the reference $[Ru(bpy)_3]^{2+}$ complex.

The luminescent behavior of the dinuclear complexes, **RuRu**, **OsOs**, and **RuOs**, is consistent with the ligand-centered triplet levels (^{3}Th) being at an intermediate energy between the ^{3}(Ru → L CT) and ^{3}(Os → L CT) levels, the latter located at ∼1.5 eV for the Os-containing species examined (according to estimates from the emission maxima of **Os**, **OsOs**, and **RuOs**, Table 2). In fact, (i) **RuRu** is not emissive, and (ii) **OsOs** and **RuOs** exibit quite similar emission efficiencies, $\phi_{em} = 3.4 \times 10^{-4}$ and 3.9×10^{-4}, respectively (Table 2). The latter emission intensity is lower than that exhibited by $[Os(bpy)_3]^{2+}$, $\phi_{em} = 3.2 \times 10^{-3}$, and **Os**, $\phi_{em} = 2.5 \times 10^{-3}$ (Table 2). This suggests that, for **OsOs** and **RuOs**, additional deactivation processes are affecting the luminescence properties, even if we have no simple explanation to offer.

It is of interest to notice that this series of complexes shows a close structural resemblance with a series of mononuclear and dinuclear complexes recently reported by us, Chart 2.[81] For the latter series, the various subunits are connected by triple bonds, instead of double bonds, and the systems can apparently to be viewed as more rigid, with the various subunits subject to a tighter electronic connections than reported here. For the Ru and Os-based complexes of Chart 2, the emission properties were attributed to excited levels of predominant MLCT nature, while for the Ru-based complexes in the present case, a predominant ligand-centered nature is proposed for the lowest-lying level, which explains the lack of luminescence. This outcome might be understood based on a comparison of the electrochemical properties of

(103) Belletete, M.; Mazerolle, L.; Desrosiers, N.; Leclerc, M.; Durocher, G. *Macromolecules* **1995**, *28*, 8587−8597.
(104) van Hal, P. A.; Knol, J.; Langeveld-Voss, B. M. W.; Meskers, S. C. J.; Hummelen, J. C.; Janssen, R. A. J. *J. Phys. Chem. A* **2000**, *104*, 5974−5988.
(105) Montalti, M.; Credi, A.; Prodi, L.; Gandolfi, M. T. *Handbook of Photochemistry*, 3rd ed.; CRC Press, Taylor & Francis: Boca Raton, FL, 2006; p 617.

Chart 2

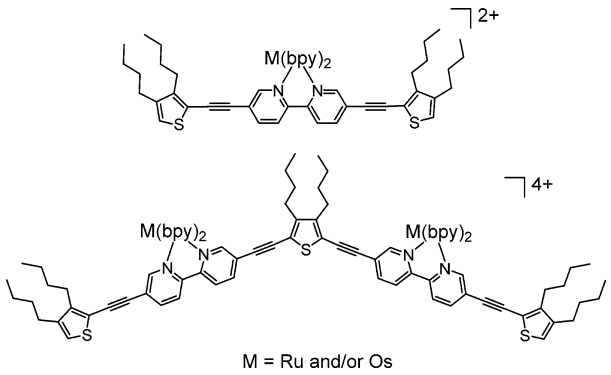

both the mononuclear and dinuclear specsies for the two series. For the complexes in the series shown in Chart 2, the "redox energies",[1] $\Delta = e(E_{ox} - E_{red})$ eV, are systematically lower than those for the series shown Chart 1. For instance, for the ruthenium dinuclear species in Chart 2, the first oxidation is at 1.32 V vs SCE, and the first reduction is at −0.99 V vs SCE;[81] $\Delta = 2.31$ eV. For the counterpart of Chart 1, the first oxidation is at 1.30 V vs SCE; the first reduction is at −1.04 V, and $\Delta = 2.34$ eV. On the basis of the well-known correlation between redox properties and MLCT levels,[1,102] this might indicate that the MLCT levels for the complexes of Chart 1 are slightly higher in energy (by ∼150−250 cm^{-1}) than those of Chart 2. Thus, it is possible that the different electronic properties of the triple and double bonds regulate the switching between closely lying ^{3}Ru → L CT and ^{3}LC(^{3}Th) levels for the complexes shown in Schemes 1 and 2.[106]

Experimental Section

Materials. The following compounds were synthesized according to the literature: 3,4-dibutyl-thiophene **1**,[90] 2-formyl-3,4-dibutyl-thiophene **1**,[91] 2,5-diformyl-3,4-dibutyl-thiophene **3**,[91] 5,5′-dimethyl-2,2′-bipyridine **4**,[93] compound **5**,[94] compound **6**,[58] *cis*-Cl-[Ru(bipy)$_2$Cl$_2$]·H$_2$O,[96] and *cis*-Cl-[Os(bipy)$_2$Cl$_2$]·H$_2$O.[97]

Electrochemical Measurements. Electrochemical studies employed cyclic voltammetry with a conventional 3-electrode system using a BAS CV-50W voltammetric analyzer equipped with a Pt microdisk (2 m^2) working electrode and a silver wire counterelectrode. Ferrocene was used as an internal standard and was calibrated against a saturated calomel reference electrode (SCE) separated from the electrolysis cell by a glass frit presoaked with electrolyte solution. Solutions contained the electroactive substrate in deoxygenated, anhydrous acetonitrile-containing tetra-*n*-butylammonium hexafluorophosphate buffer(0.1 M) as supporting electrolyte. The quoted half-wave potentials were reproducible within ∼15 mV.

Optical Spectroscopy. The absorption spectra of dilute solutions (2×10^{-5} M) of CH_2Cl_2 (for the ligands) and CH_3CN (for the complexes) were obtained with a Perkin-Elmer Lambda 45 UV−vis spectrometer. The luminescence spectra for air-equilibrated solutions at room temperature (absorbance <0.15 at the excitation wavelength) and at 77 K were measured using an Edinburgh FLS920 spectrometer equipped with a Hamamatsu R5509-72 supercooled photomultiplier tube (193 K), a TM300 emission monochromator with NIR grating blazed at 1000 nm, and an Edinburgh Xe900 450 W xenon arc lamp as light source. The excitation wavelengths were 400 and 450 nm for the ligands and complexes, respectively. Corrected luminescence spectra in the range of 700−1800 nm were obtained by using a correction curve for the phototube response provided by the manufacturer. Luminescence quantum efficiencies (ϕ_{em}) were evaluated by comparison of the wavelength-integrated intensities (I) with reference to [Ru(bpy)$_3$]Cl$_2$ ($\phi_r = 0.028$ in air-equilibrated water)[107] or [Os(bpy)$_3$](PF$_6$)$_2$ ($\phi_r = 0.005$ in degassed acetonitrile)[102] as standards using the equation[102,108]

$$\phi_{em} = \frac{A_r \eta^2 I}{\eta_r^2 I_r A} \phi_r \qquad (1)$$

where A and η are absorbance values (<0.15) at the employed excitation wavelength and refractive index of the solvent, respectively. Band maxima and relative luminescence intensities are obtained with uncertainty of 2 nm and 20%, respectively. The luminescence lifetimes of the complexes were obtained with the same equipment operated in single-photon mode with a 407 nm laser diode excitation controlled by a Hamamatsu C4725 stabilized picosecond light pulser. For the ligand lifetimes, an IBH 5000F single photon device was employed, with excitation at 373 nm. Analysis of the luminescence decay profiles against time was accomplished with the software provided by the manufacturers. Estimated errors are 10% on lifetimes, 20% on quantum yields, and the working temperature was either 298 ± 2 K (1 cm^2 optical cells employed) or 77 K (with samples contained in capillary tubes immersed in liquid nitrogen).

Syntheses. General Procedure 1: Horner−Wadsworth−Emmons Olefination. A suspension of potassium *tert*-butoxide was added dropwise to a mixture of aldehyde, phosphonate, and THF. The mixture was stirred at room temperature for 1 h. After extraction with dichloromethane, the organic fractions were washed with water, dried over absorbent cotton, and evapored in vacuo. The residue was purified by chromatography on alumina, eluting with petroleum ether−dichloromethane (1/3, v/v), and was recrystallized from dichloromethane−cyclohexane.

Ligand 7 (monomer). Ligand **7** was prepared using General Procedure 1 from **6** (153 mg, 0.3 mmol), **2** (151 mg, 0.7 mmol) in anhydrous THF (4 mL), and *t*-BuOK (75 mg, 0.67 mmol) in anhydrous THF (4 mL) for 1 h to give 172 mg of **7** (96%) as a yellow solid. mp: 150(1) °C. ^{1}H NMR (200 MHz, $CDCl_3$): δ 8.73 (d, 2H, $^4J = 2.0$ Hz), 8.38 (d, 2H, $^3J = 8.3$ Hz), 7.88 (dd, 2H, $^4J = 2.0$ Hz, $^3J = 8.3$ Hz), 7.12 (AB, 4H, $J_{AB} = 15.8$ Hz, $\nu o\delta = 98.7$ Hz), 6.83 (s, 2H), 2.67 (t, 4H, $^3J = 7.3$ Hz), 2.51 (t, 4H, $^3J = 7.7$ Hz), 1.44 (m, 16H), 0.97 (t, 12H, $^3J = 6.9$ Hz). ^{13}C NMR (50 MHz, $CDCl_3$): δ 154.3, 147.7, 143.4, 141.4, 136.3, 133.2, 133.1, 123.1, 122.9, 120.8, 119.2, 33.4, 31.8, 28.7, 26.8, 22.8, 22.6, 13.9. IR (KBr, cm^{-1}): ν 3022, 2997, 2947, 2928, 2863, 1616, 1466, 1453, 1374. UV−vis (CH_2Cl_2) λ, nm (ϵ, M^{-1} cm^{-1}): 286 (11 500), 398 (67 000). FAB$^+$ (nature of the peak, relative intensity): *m*/*z* 597.2 ([M + H]$^+$, 100). Anal. Calcd for $C_{38}H_{48}N_2S_2$: C, 76.46; H, 8.10; N, 4.69. Found: C, 76.19; H, 7.79; N, 4.45.

Compound 8. Compound **8** was prepared following General Procedure 1 from **6** (524 mg, 1.1 mmol), **2** (259 mg, 1.1 mmol) in anhydrous THF (8 mL), and *t*-BuOK (130 mg, 1.1 mmol) in anhydrous THF (4 mL) for 1 h to give 284 mg of **8** (49%) as a pale yellow solid. ^{1}H NMR (200 MHz, $CDCl_3$): δ 8.69 (m, 1H),

(106) The lowest-energy absorption properties are not helpful in the cases under scrutiny because of the overlapping of the ^{1}MLCT transitions (expected to correlate with the redox properties) and the stronger ligand-centered transitions, see text.

(107) Nakamaru, K. *Bull. Chem. Soc. Jpn.* **1982**, *55*, 2967.
(108) Demas, J. N.; Crosby, G. A. *J. Phys. Chem.* **1971**, *75*, 991.

8.55 (m, 1H), 8.35 (m, 2H), 7.88−7.73 (m, 2H), 7.10 (AB, 1H, J_{AB} = 16.0 Hz, $\nu o\delta$ = 99.1 Hz, E diastereoismer), 6.82 (s, 1H), 6.61 (AB, 1H, J_{AB} = 12.1 Hz, $\nu o\delta$ = 44.9 Hz, Z diastereoismer), 4.05 (m, 4H), 3.19 (d, 2H, $^2J_{HP}$ = 21.5 Hz), 2.64 (t, 2H, ^3J = 7.1 Hz), 2.48 (t, 2H, ^3J = 7.8 Hz), 1.63−1.18 (m, 14H), 0.96 (m, 6H). FAB^+ (nature of the peak, relative intensity): *m*/*z* 527.2 ($[M + H]^+$, 100). Anal. Calcd for $C_{29}H_{39}N_2SPO_3$: C, 66.13; H, 7.46; N, 5.32. Found: C, 65.85; H, 7.17; N, 5.14.

Ligand 9 (dimer). Ligand **9** was prepared following General Procedure 1 from **8** (50 mg, 0.1 mmol), **3** (11 mg, 0.05 mmol) in anhydrous THF (7 mL), and *t*-BuOK (10 mg, 0.09 mmol) in anhydrous THF (8 mL) for 2 h to give 42 mg of **9** (84%) as a orange-red solid. mp: 186(7) °C. ^{1}H NMR (300 MHz, $CDCl_3$): δ 8.73 (s, 4H), 8.38 (dd, 4H, ^3J = 8.5 Hz, ^4J = 1.6 Hz), 7,88 (d, 4H, ^3J = 8.3 Hz), 7.37 (d, 2H, ^3J = 16.1 Hz), 7.36 (d, 2H, ^3J = 15.9 Hz), 6.90 (d, 2H, ^3J = 15.8 Hz), 6.86 (d, 2H, ^3J = 16.1 Hz), 6.83 (s, 2H), 2,66 (t, 8H, ^3J = 7.4 Hz), 2.51 (t, 4H, ^3J = 7.4 Hz), 1.46 (m, 24H), 0.98 (m, 18H). ^{13}C NMR (50 MHz, $CDCl_3$): δ 154.4, 154.2, 147.8, 147.7, 143.4, 142.8, 141.4, 136.3, 135.5, 133.2, 133.1, 132.9, 124.1, 123.1, 122.9, 122.1, 120.8, 119.2, 33.6, 33.3, 31.8, 28.7, 26.9, 26.8, 22.9, 22.8, 22.6, 14.0. IR (KBr, cm^{-1}): ν 3027, 2952, 2929, 2859, 1618, 1466, 1376. UV−vis (CH_2Cl_2) λ, nm (ϵ, M^{-1} cm^{-1}): 284 (18 000), 454 (105 000). FAB^+ (nature of the peak, relative intensity): *m*/*z* 527.2 ($[M + H]^+$, 100); Anal. Calcd for $C_{64}H_{76}N_4S_3$: C, 77.06; H, 7.68; N, 5.62. Found: C, 76.80; H, 7.41; N, 5.17.

General Procedure 2: Ru or Os Complexation. A Schlenk flask was charged with the ligand, *cis*-Cl6[$Ru(bipy)_2Cl_2$]·H_2O or *cis*-Cl6[$Os(bipy)_2Cl_2$]·H_2O, and finally, ethyl alcohol. The solution was heated at 90 °C until complete consumption of starting material. At the end of the reaction, the solvent was removed, and 4 mL of a saturated aqueous solution of KPF_6 was added. After 3 extractions with dicloromethane, the organic phase was dried over absorbent cotton. The solvent was removed. The crude product was purified by chromatography on alumina, eluting with dichloromethane-methanol (98/2, v/v), and was recrystallized from dichloromethane−cyclohexane.

Compound 10a (Ru). Compound **10a** was prepared following General Procedure 2 from **7** (40 mg, 0.07 mmol), $Ru(bipy)_2Cl_2$ (38 mg, 0.08 mmol), and ethanol (8 mL) for 14 h to give 64 mg (70%) of **10a** as a brown solid. mp: 281(2) °C. ^{1}H NMR (300 MHz, $(CD_6)CO$): δ 8.77 (m, 4H), 8.65 (d, 2H, ^3J = 8.7 Hz), 8.43 (dd, 2H, ^3J = 8.6 Hz, ^4J = 1.8 Hz), 8.22−8.08 (m, 10H) 7.54 (m, 6H), 7.03 (s, 2H), 6.59 (d, 2H, ^3J = 16.0 Hz), 2.64 (t, 4H, ^3J = 7.2 Hz), 2.49 (t, 4H, ^3J = 7.6 Hz), 1.45 (m, 16H), 0.90 (m, 12H). ^{13}C NMR (50 MHz, $CDCl_3$): δ 158.2, 155.6, 152.8, 152.7, 150.8, 144.4, 144.1, 138.85, 138.81, 137.9, 136.5, 133.8, 128.7, 128.6, 127.1, 125.32, 125.27, 124.8, 122.0, 121.3, 34.2, 32.6, 27.0, 23.24, 23.18, 14.3, 14.2. IR (KBr, cm^{-1}): ν 3022, 2952, 2930, 2870, 1615, 1596, 1465, 1446, 1384. UV−vis (CH_2Cl_2) λ, nm (ϵ, M^{-1} cm^{-1}): 288 (74 500), 459 (70 500). ES-MS positive mode, CH_3CN (nature of the peak, relative intensity): *m*/*z* 1155.2 ($[M- PF_6]^+$, 100), 505.2 ($[M- 2PF_6]^{2+}$, 60). Anal. Calcd for $C_{58}H_{64}N_6S_2RuP_2F_{12}$: C, 76.98; H, 7.48; N, 4.72. Found: C, 76.52; H, 7.18; N, 4.40.

Compound 10b (Os). Compound **10b** was prepared following General Procedure 2 from **7** (40 mg, 0.07 mmol), $Os(bipy)_2Cl_2$ (42 mg, 0.08 mmol), and ethanol (8 mL) for 2 days to give 46 mg (47%) of **10b** as a bright black solid. mp: 287(8) °C. ^{1}H NMR (300 MHz, $(CD_6)_2CO$): δ 8.78 (m, 4H), 8.67 (d, 2H, ^3J = 8.9 Hz), 8.30 (dd, 2H, ^3J = 8.7 Hz, ^4J = 1.5 Hz), 8.02 (m, 10H), 7.53 (m, 6H), 7.05 (s, 2H), 6.61 (d, 2H, ^3J = 16.1 Hz), 2.68 (t, 4H, ^3J = 7.3 Hz), 2.52 (t, 4H, ^3J = 7.3 Hz), 1.61 (m, 4H), 1.43 (m, 12H), 0.92 (t, 6H, ^3J = 7.3 Hz), 0.88 (t, 6H, ^3J = 7.1 Hz). ^{13}C NMR (50 MHz, $CDCl_3$): δ 160.2, 157.5, 152.0, 151.8, 150.1, 144.4, 144.2, 138.5, 138.2, 136.4, 133.0, 129.2, 129.1, 127.4, 125.6, 125.5, 124.9, 122.2, 121.0, 34.2, 32.7, 23.24, 23.18, 14.3, 14.2. IR (KBr, cm^{-1}): ν 3025, 2947, 2929, 2869, 1615, 1592, 1464, 1443, 1384. UV−vis (CH_2Cl_2) λ, nm (ϵ, M^{-1} cm^{-1}): 292 (71 000), 467 (60 000). ES-MS positive mode, CH_3CN (nature of the peak, relative intensity): *m*/*z* 1245.2 ($[M- PF_6]^+$, 100), 550.1 ($[M- 2PF_6]^{2+}$, 35). Anal. Calcd for $C_{58}H_{64}N_6S_2OsP_2F_{12}$: C, 50.14; H, 4.64; N, 6.05. Found: C, 49.79; H, 4.29; N, 5.68.

Compound 11a (RuRu). Compound **11a** was prepared following General Procedure 2 from **9** (35 mg, 0.04 mmol), $Ru(bipy)_2Cl_2$ (28 mg, 0.06 mmol), and ethanol (8 mL) for 16 h to give 63 mg (65%) of **11a** as a brown solid. mp: >300 °C. ^{1}H NMR (300 MHz, $(CD_6)_2CO$): δ 8.80−8.65 (m, 12H), 8.48 (m, 4H), 8.31−8.05 (m, 20H), 7.59 (m, 12H), 7.07 (s, 2H), 6.62 (d, 2H, ^3J = 15.8 Hz), 6.60 (d, 2H, ^3J = 15.8 Hz), 2.67 (m, 8H), 2.52 (t, 4H, ^3J = 7.7 Hz), 1.62−1.26 (m, 24H), 0.91 (t, 18H). IR (KBr, cm^{-1}): ν 3023, 2952, 2929, 2868, 1611, 1592, 1465, 1446, 1374. UV−vis (CH_2Cl_2) λ, nm (ϵ, M^{-1} cm^{-1}): 288 (113 000), 526 (57 000), 566 (40 000). ES-MS positive mode, CH_3CN (nature of the peak, relative intensity): *m*/*z* 2259.3 ($[M- PF_6]^+$, 20), 656.6 ($[M- 3PF_6]^{3+}$, 65), 456.2 ($[M- 4PF_6]^{4+}$, 100). Anal. Calcd for $C_{104}H_{108}N_{12}S_3Ru_2P_4F_{24}$: C, 51.95; H, 4.53; N, 6.99. Found: C, 51.58; H, 4.29; N, 6.73.

Compound 11b (OsOs). Compound **11b** was prepared following General Procedure 2 from **9** (70 mg, 0.08 mmol), $Os(bipy)_2Cl_2$ (62 mg, 0.10 mmol), and ethanol (8 mL) for 2 days to give 74 mg of **11b** (36%). mp: >300 °C. IR (KBr, cm^{-1}): ν 3028, 2954, 2928, 2867, 1607, 1589, 1463, 1421, S1374. UV−vis (CH_2Cl_2) λ, nm (ϵ, M^{-1} cm^{-1}): 291 (145 000), 506 (79 000), 554 (57 000). ES-MS positive mode, CH_3CN (nature of the peak, relative intensity): *m*/*z* 2439.5 ($[M - PF_6]^+$, 80), 501.2 ($[M - 4PF_6]^{2+}$, 10). Anal. Calcd for $C_{104}H_{108}N_{12}S_3Os_2P_4F_{24}$: C, 48.37; H, 4.22; N, 6.51. Found: C, 48.02; H, 3.89; N, 6.17.

Compound 12 (RuOs): Compound **12** was prepared following General Procedure 2 from the mono-osmium complex of ligand **9** (44 mg, 0.01 mmol), $Ru(bipy)_2Cl_2$ (6 mg, 0.02 mmol), and ethanol (8 mL) for 2 days to give 34 mg of **12** (69%) as a bright black solid. mp: >300 °C. UV−vis (CH_2Cl_2) λ, nm (ϵ, M^{-1} cm^{-1}): 290 (98 700), 456 (55 000), 563 (31 000). ES-MS positive mode, CH_3CN (nature of the peak, relative intensity): *m*/*z* 478.5 ($[M- 4PF_6]^{2+}$, 80). Anal. Calcd for $C_{104}H_{108}N_{12}S_3RuOsP_4F_{24}$: C, 50.10; H, 4.37; N, 6.74. Found: C, 49.79; H, 4.12; N, 6.73.

Acknowledgment. This research was supported by the CNRS, le Ministère de la Recherche et des Nouvelles Technologies, by the CNR project PM-P03-ISTM-C4/PM-P03-ISOF-M5 (Componenti molecolari e supramolecolari o macromolecolari con proprietà fotoniche ed optoelettroniche), and by the FIRB project RBNE019H9K "Molecular Manipulation for Nanometric Devices" of MIUR.

IC061825Y